



Journal Homepage: - www.journalijar.com

INTERNATIONAL JOURNAL OF ADVANCED RESEARCH (IJAR)

Article DOI: 10.21474/IJAR01/23380

DOI URL: <http://dx.doi.org/10.21474/IJAR01/23380>



RESEARCH ARTICLE

BATCH ADSORPTION OF OFLOXACIN ONTO ACTIVATED CARBON DERIVED FROM EGGSHELLS

Odi Assemien Prisca Elodie¹, Soro Donafologo Baba¹, N'zueyojeanvianney¹, Yaya Coulibaly², Acho Yapifulgence¹, N'guettiakossonouroland¹, Aboua Kouassi Narcisse¹, Meite Ladji¹ and Traore Karim Sory¹

1. Laboratory of Environmental Sciences, Faculty of Environmental Sciences and Management, Nangui ABROGOUA University, 02 BP 801 Abidjan 02, Côte d'Ivoire.

2. Faculty of Agriculture, Fisheries Resources and Agro-industries, University of SAN-PEDRO, 01 BP 1800 SAN-PEDRO 01, Côte d'Ivoire.

Manuscript Info

Manuscript History

Received: 15 February 2026

Final Accepted: 18 March 2026

Published: April 2026

Key words:-

Adsorption, Ofloxacin, Activated carbon; Eggshells

Abstract

The aim of this study is to investigate the potential of eggshells as a precursor for activated carbon in the removal of ofloxacin from aqueous media. The dried eggshells were ground, and particle size separation was used to retain particles with diameters between 1 and 2 mm. This ground material was activated with 30% orthophosphoric acid at a ratio of 0.5 and then calcined at 600 °C in an oven for 1 hour. Characterisation tests were carried out to determine the iodine index, specific surface area, surface functions, and pH_{zpc}. During the adsorption tests, the residual concentrations of ofloxacin were monitored using a high-performance liquid chromatograph (HPLC). The contact time, mass of activated carbon, pH, and initial concentration of the pollutant were varied for the removal of ofloxacin. The adsorption kinetics were modelled. The results reveal that the prepared activated carbon has an iodine index of 450.85 mg/g and a specific surface area of 5.29 m²/g, and is predominantly mesoporous. It is basic in nature, with a pH_{zpc} value of 7.4. The adsorption of ofloxacin is optimal (65.75%) at a pH of 6, a carbon mass of 8 g, an initial concentration of 20 mg/L, and a contact time of 90 minutes. The pseudo-second-order model and the Langmuir and Dubinin-Radushkevich isotherm models are suitable for describing the adsorption process.

"© 2026 by the Author(s). Published by IJAR under CC BY 4.0. Unrestricted use allowed with credit to the author."

Introduction:-

The pollution of water resources caused by human activities has become an issue to which the whole world now attaches great importance. The growing presence of pharmaceutical residues in aquatic ecosystems has become a major environmental concern (Bound and Voulvoulis, 2005). Among the substances present in the aquatic environment are fluoroquinolones, which belong to a class of antibiotics of significant concern as they are the most widely produced and used. These antibiotics are widely used in aquaculture, agriculture, and human and veterinary medicine (Guo et al., 2013). Ofloxacin, an antibiotic from the fluoroquinolone family, is frequently detected in

Corresponding Author:- Odi Assemien Prisca Elodie

Address:- Laboratory of Environmental Sciences, Faculty of Environmental Sciences and Management, Nangui ABROGOUA University, 02 BP 801 Abidjan 02, Côte d'Ivoire.

hospital and urban effluents due to its incomplete metabolism by the human body (Kummerer, 2009). Its presence contributes to acute and chronic toxicity towards aquatic microflora as well as the emergence of resistant bacteria. Ofloxacin, as a broad-spectrum antibacterial agent, is increasingly used in the treatment and prevention of various diseases (Garcia et al., 2019). Given that its persistence in the environment can cause adverse effects on aquatic ecosystems and human health, ofloxacin has attracted increasing attention (Leipert et al., 2018). It is therefore necessary to develop effective treatment options to reduce the release of these pollutants into the environment.

Conventional treatment processes have been tested for the removal of pharmaceutical residues, such as Fenton oxidation (Gupta and Garg, 2018), Photo-Fenton oxidation (Giri and Golder, 2015), photochemical degradation (Guo et al., 2013), ozonation (Liu et al., 2012) and adsorption (Shi et al., 2013). In response to this challenge, adsorption is widely recognised as a technique of choice due to its high efficiency, ease of implementation and ability to treat highly diluted solutions (Ahmad et al., 2014). Activated carbon is widely used as an adsorbent due to its large surface area, micro/mesoporous nature and high adsorption capacity, without producing toxic or pharmacologically active compounds (Rivera et al., 2013). However, the high cost of commercial activated carbon is prompting current research to turn towards alternative and renewable precursors. The recovery of waste materials such as eggshells forms part of a circular economy approach. It is within this context that this study is situated, the objective of which is to test the efficacy of activated carbon prepared from eggshells for the adsorption of ofloxacin in an aqueous medium.

Materials and Methods:-

Solvents and reagents:-

The main solvents and reagents used are ofloxacin (OFL) of 98% purity, belonging to the fluoroquinolone class of therapeutic agents, supplied by Sigma Aldrich. Its chemical structure is shown in Figure (1). The acetonitrile and formic acid used for chromatographic analyses are of analytical grade or higher and are supplied by Prolabo and Carlo Erbra respectively.

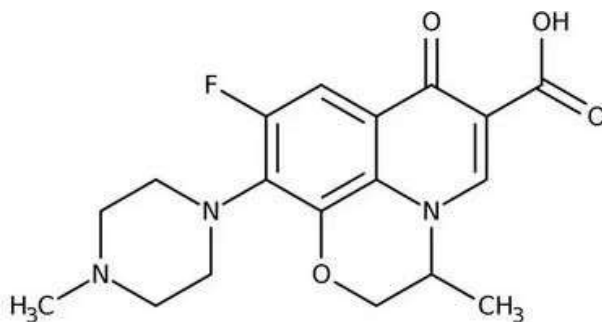


Figure 1: Chemical structure of OFL

Preparation of activated carbon:-

The eggshells, used as a precursor, were collected from egg sellers in the city of Abidjan, Côte d'Ivoire. They were washed several times with tap water and boiling water, then rinsed with distilled water to remove impurities. They were then dried at 110 °C for 24 hours in a Memmert oven. Subsequently, they were ground and sieved to extract the fraction of particles of uniform size between 1 and 2 mm. These samples were impregnated for 24 hours in a 50% orthophosphoric acid solution, dried in the oven and then calcined at 600 °C for 1 hour in a Nabertherm muffle furnace with a heating rate of 10 °C/min. The resulting carbonised material (CAO) was washed several times with distilled water until the pH of the wash water was neutral. It was dried in an oven at 110 °C for 24 hours.

Characterisation Of Activated Carbon:-

Ash content (AC):-

To determine this content, a porcelain crucible was preheated to 700 °C for 10 minutes and its mass was measured after cooling. The dry carbon was placed in the crucible and the assembly was heated to 700 °C for 3 hours. The mass of the assembly was determined and the ash content was calculated using the following equation:

$$\text{TC (\%)} = \frac{m_3 - m_1}{m_2 - m_1} * 100 \quad (1)$$

where:

m_1 : Mass of the crucible (g);

m_2 : Mass of the crucible plus charcoal (g);

m_3 : Mass of crucible plus coal after heating (g).

SURFACE FUNCTIONS:-

Surface functions were quantified using the Boehm method by titration with NaOH and HCl. Basic groups are titrated as a whole, whilst acidic groups are titrated separately using bases of increasing strength. A mass of 0.4 g of activated carbon is mixed with 20 mL of one of the following acidic or basic compounds at a concentration of 0.1 M : NaHCO₃, Na₂CO₃, NaOH and HCl. The mixture is stirred for 24 hours and then filtered. A 10 mL volume of the filtrate is taken and titrated with 0.1 M NaOH or 0.1M HCl, as appropriate.

The amount of basic functional groups was obtained directly from the back titration; that of the acidic groups was estimated by making the following assumptions:

- The NaOH solution neutralises the carboxylic, phenolic and lactone groups;
- The Na₂CO₃ solution neutralises the carboxylic and lactone groups;
- The NaHCO₃ solution neutralises the carboxylic groups.

pH at the zero-charge point (pHpzc):-

In accordance with the protocol proposed by Rivera et al. (2013), 0.15 g of charcoal was added to 50 mL of a 0.01 M NaCl solution with a pH ranging from 2 to 12. The pH was adjusted using a 0.01 M HCl solution and a 0.01 M NaOH solution. The suspensions were then stirred for 24 hours at room temperature, after which the final pH (pH_f) was measured. We then plot ΔpH (pH_f – pH_i) against the initial pH of the solution (pH_i). The intersection of this curve with the x-axis gives the pH value at the zero-charge point.

Elemental analysis:-

This analysis was carried out using approximately 100 mg of charcoal. The main elements determined are the contents of oxygen (O), carbon (C), nitrogen (N), sulphur (S) and hydrogen (H), as well as exchangeable ions, such as calcium (Ca²⁺), sodium (Na⁺), potassium (K⁺) and magnesium (Mg²⁺) ions. The samples are placed on a surface known as a pad, 12 cm in diameter. The assembly is then adjusted under the microscope so that the entire surface of the pad is covered with charcoal grains, and then passed through a Q150-RS metalliser. The data obtained are given as % by weight.

Fourier Transform Infrared Spectroscopy (FTIR):-

The analysis was carried out using a Nicolet iS50 FTIR Fourier transform spectrometer (ThermoFisher Scientific) coupled with a digital computer to plot the spectra, which were then processed using OMNIC software. To perform this test, 1 mg of sample is mixed with 100 mg of potassium bromide (KBr). The mixture is then compressed under a uniaxial pressure of 350 MPa and dried for 48 hours at 105°C. This type of preparation allows the most intense vibration bands of the material to be analysed, under ex situ conditions only, without detector saturation. This enabled the acquisition of FTIR spectra (transmittance % as a function of wavenumber in cm⁻¹).

Specific surface area and porosity:-

BET specific surface area:- The specific surface area of the activated carbon was measured using a Micromeritics TRISTAR 2 instrument with nitrogen (N₂) as the gas. Using this method, nitrogen adsorption isotherms at 77 K (the boiling point of liquid nitrogen) were established. It is based on the BET model, validated at low relative pressures (0.05 ≤ P/P₀ ≤ 0.35). By assigning the nitrogen molecule a surface area S_p = 16.2 × 10⁻²⁰m² and using all data taken from the CNTP, the specific surface area (SBET) is given by the equation below:

$$S_{\text{BET}} (\text{m}^2/\text{g}) = S_p \left(V_m \frac{N}{V_{\text{molaire}}} \right) = 4,35.10^6 V_m \quad (2)$$

Where:

N: Avogadro's number (6.025 × 10²³ mol⁻¹)

V_m: volume required to saturate a monolayer (m³/g)

Porosity:-

The study of porosity was carried out using the t-method or t-plot (Lippens et al., 1965). This involves plotting the volume of gas adsorbed per gram of solid (in cm³/g) at relative pressure P/P₀ against the statistical thickness t (in Å) of the layer

adsorbed on the non-porous reference solid at that same relative pressure. The number of molecular layers adsorbed at pressure P on the solid is determined by calculating the ratio of the volume V of vapour adsorbed at each pressure P to the volume required for the saturation of a monolayer (V_m) calculated using the surface area equation (SBET). The thickness t is obtained by multiplying this ratio (V/V_m) by the statistical thickness of a monomolecular layer (e) according to the following relationship:

$$t = \left(\frac{V}{V_m}\right) e = \frac{e p_o}{p_o - p} \quad (3)$$

Adsorption Experiments:-

Parametric study:-

Effect of contact time:-

To study the contact time, 8 g of CAO were suspended in a 500 mL solution of OFL with a concentration $C_0 = 20$ mg.L⁻¹ at a stirring speed of 250 rpm.

Effect of adsorbent dose:-

The effect of the adsorbent dose was studied by bringing different masses of CAO (8 g; 10 g; 12 g; 14 g and 15 g) into contact with 500 mL of OFL solution with a concentration of $C_0 = 20$ mg.L⁻¹.

Effect of pH:-

The effect of the initial pH of the solution was investigated by introducing 14 g of CAO into 500 mL of OFL solution at a concentration of 20 mg.L⁻¹. The pH of the solutions was first adjusted to the following values: 5; 6; 7; 9; 10, by adding a few drops of 0.1 M concentrated HCl or NaOH solutions.

Modelling of adsorption kinetics:-

The kinetic modelling of OFL adsorption was carried out using the following four models (linear form):

✓ Pseudo-first-order kinetic model: $\ln(Q_e - Q_t) = \ln Q_e - k_1 t$ (Weng and Huang, 2004) (4)

✓ Pseudo-second-order kinetic model:

$$(5) \quad \frac{t}{Q_t} = \frac{1}{K_2 Q_e^2} + \frac{1}{Q_e} t \quad (\text{Horsfall and Spiff, 2004})$$

✓ Elovich kinetic model:

$$Q_t = \frac{1}{\beta} \ln t + \frac{1}{\beta} \ln(\alpha \cdot \beta) \quad (\text{Fierro et al., 2008}) \quad (6)$$

✓ Intraparticle diffusion kinetic model:

$$(7) \quad Q_t = k_{int} t^{1/2} + C \quad (\text{Omokpariola, 2021})$$

K_1 (min⁻¹), K_2 (g/mg·min), α (mg/mg·min), β (g/mg) and K_{int} (mg/g min^{-1/2}) are, respectively, the pseudo-first-order, pseudo-second-order, Elovich and intraparticle diffusion kinetic constants.

Modelling of adsorption isotherms:-

The study of adsorption isotherms enables the determination of the adsorption capacity of the adsorbates (OFL) on the adsorbent, as well as the type of adsorption mechanism. Three adsorption isotherm models were used in this study in their linear forms:

➤ Langmuir:

$$\frac{C_e}{Q_e} = \frac{1}{b Q_m} + \frac{1}{Q_m} C_e \quad (\text{Avom et al., 2001}) \quad (8)$$

The separation factor R_L is determined by the following relationship:

➤ Freundlich : $Q_e = K_F C_e^{1/n}$ [(Al Mardini, 2008) (9)

$$R_L = 1/(1 + K_L C_e)$$

➤ Dubinin-Radushkevich :

$$\ln(Q_e) = \ln(q_m) - \beta \varepsilon^2 \quad (\text{Samarghandi et al., 2009}) \quad (10)$$

The Polanyi ε potential is determined by the following equation:

$$\varepsilon = R T \ln \left(1 + \frac{1}{C_e}\right)$$

Results and Discussion:-

Characterisation of activated carbon:-

Ash content:-

Activated carbon derived from eggshells (ACE) has a very high ash content of 94.40%. This indicates that the materials have a low carbon content and are therefore rich in inorganic matter. Eggshells consist mainly of calcium carbonate, calcium oxides, magnesium and potassium (Adeyeye, 2009; Mohadi et al., 2016).

Surface activity and pH at the zero-charge point (pHzpc) :-

The surface functions of the CAO and the determined pHzpc are presented in Table (1). In view of these results, the CAO exhibits basic properties generally attributed to the presence of pyrone groups and ash content (Fingueneisel, 1998), with an average total basicity of 4.96 meq/g compared with an average total acidity of 3.21 meq/g.

Table (1): Concentrations of surface functions (meq/g) and pHzpc

Function carboxylic	Function phénolic	Function lactonic	Total base	Total acid	pHzpc	Character surface
1.53	1.64	0.04	4.96	3.21	7.40	basic

According to this table, CAO consists mainly of carbon (11.33%), phosphorus (5.39%), calcium (30.78%) and oxygen (50.53%). Such results were reported by Habeeb et al. (2014). These results reveal that the activated carbon prepared consists mainly of oxygen. This suggests the presence of oxygen-containing groups, such as acidic groups. Chicken eggshells consist of more than 95% calcium carbonate. This is further confirmed by their high calcium content. The presence of phosphorus in the material could be explained by the fact that, during activation with phosphoric acid, phosphorus atoms bond with carbon atoms to form bridges between the carbon atoms, thereby creating or enlarging the pores (Nahil and Williams, 2012).

Fourier Transform Infrared Spectroscopy (FTIR):-

Figure (2) shows the spectra obtained by infrared spectroscopy of both raw coal (COB) and 30% activated coal (CAO 30%), measured between 650 and 4,000 cm^{-1} . The COB spectrum is dominated by narrow, intense bands, typical of the vibrations of carbonate groups at 1792.1, 1393.0, 871.5 and 712.3 cm^{-1} . These are characteristic bands of calcium carbonate (CaCO_3) (Farcas and Touzé, 2001). The band observed at 1792.1 cm^{-1} corresponds to stretching vibrations often attributed to a specific combination band in carbonates (Brečević and Nielsen, 1990). The very intense band at 1393.0 cm^{-1} is the main signature of the asymmetric C–O stretching vibration of the carbonate group (Skoog et al., 2018). The narrow bands at 871.5 cm^{-1} and 712.3 cm^{-1} are attributed respectively to out-of-plane and in-plane deformation of the carbonate group, confirming the mineral structure (Pilecki et al., 2019). The spectrum of 30% CAO shows almost complete overlap with the COB spectrum. Consequently, no significant variation in intensity, nor disappearance of the observed bands or appearance of new bands, is observed in the COB spectrum. These results show that activation has no major impact on the surface functional groups of CAO. The involvement of functional groups in the adsorption of OFL is similar between COB and activated CAO, and governed by other factors such as porosity.

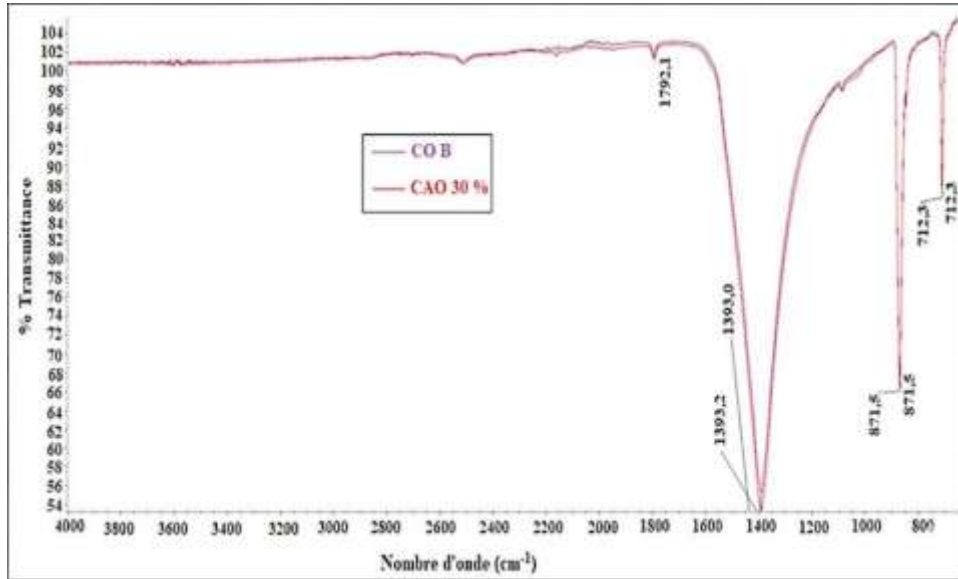


Figure 2 : FTIR transmission spectra of the samples

Specific surface area and porosity:-

Figure (3) shows the N₂ adsorption-desorption isotherms at 77 K for CAO. According to the IUPAC classification of adsorption-desorption isotherm curves, the curves obtained are of type IV, indicating that adsorption occurs in several stages, a characteristic of mesoporous materials. The presence of a hysteresis loop between the adsorption and desorption curves confirms the mesoporous structure, which allows for physical adsorption at the surface. The nitrogen (N₂) adsorption isotherms also provide information on the pore volume. These results show that the pore volume obtained by nitrogen adsorption is predominantly mesoporous. It has a specific surface area of 5.429 m²/g and a pore volume of 0.030 cm³/g. This can be attributed to the dominant mineral composition of eggshells, consisting mainly of calcium carbonate, which determines the mechanisms of thermal decomposition and porosity creation during activation. Although the specific surface area of these materials is generally lower, their more open porosity can facilitate the diffusion of the adsorbate to the internal active sites.

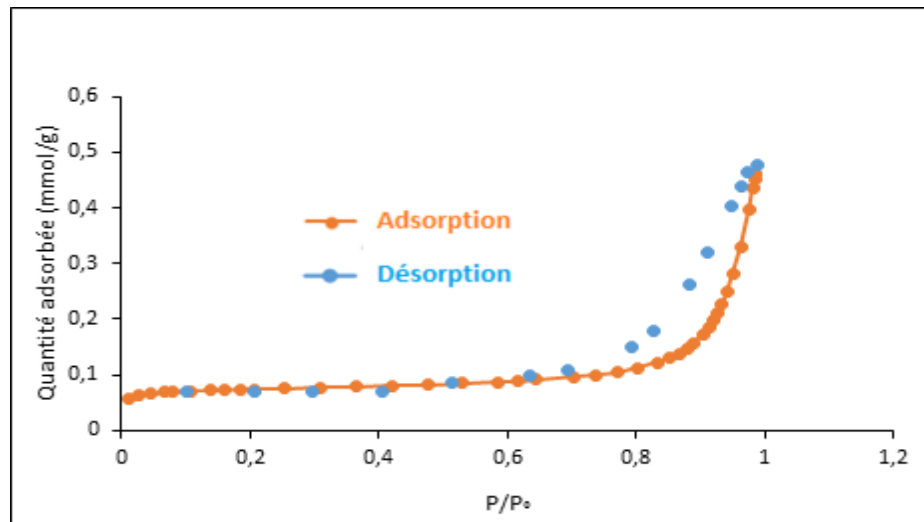


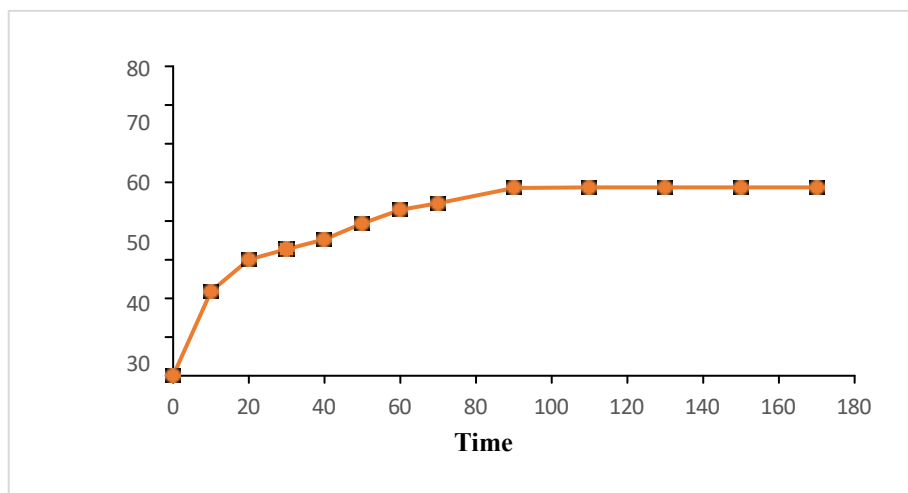
Figure 3: Adsorption and desorption isotherms of N₂ on CAO 50%

Table 3. Specific surface area and pore properties of the carbon

Specific surface area (m^2/g)	BET	5.429
Pore volume (cm^3/g)	Single-point adsorption	0.03
Microporous volume (cm^3/g)	t-Plot	0.001
Mesopore volume (cm^3/g)	BJH adsorption BJH desorption	0.029

Adsorption tests:-**Effect of contact time:-**

Figure (4) shows the evolution of the adsorption rate of ofloxacin on CAO as a function of time. This curve can be divided into three parts. Adsorption is rapid during the first twenty minutes, with an adsorption rate of 30%. This rapid increase in the adsorption rate of OFL on CAO could be explained by the presence of a large number of available sites on the adsorbent. However, it could also be linked to the physicochemical characteristics of the material and, in particular, to the nature of its porosity (Aboua, 2013). The second, slower phase is observed from 20 min to 90 min, corresponding to 48.54% removal. The slow adsorption phase observed is thought to be due to internal mass transfer within the adsorbent. This generally corresponds to a diffusion phenomenon within the internal porosity of the adsorbent (Creangă, 2007). The number of free sites decreases over time, thereby causing a slowdown in adsorption. Beyond this time interval, a plateau is reached, corresponding to the third phase. The plateau is thought to be due to the fact that the adsorbent-adsorbate interaction has reached equilibrium, i.e. saturation of the binding sites on the adsorbents

Figure 4: Effect of contact time on the adsorption of OFL, $C_0 = 20 \text{ mg/L}$; $V = 500 \text{ mL}$; $\text{pH} = 6$ **Effect of adsorbent dose:-**

The characteristic curve showing the effect of adsorbent dose on OFL adsorption is presented in Figure (5). The figure shows a decrease in the amount adsorbed per unit mass (0.6 to 0.45 mg/g) as the mass of the adsorbent increases (8 to 15 g). This could be explained by the non-saturation of adsorption sites on the activated carbons (Patil and Shrivastava, 2010). Indeed, an increase in the amount of adsorbent increases the number of available adsorption sites on its surface for a given adsorbate concentration. Thus, the mass of activated carbon increases proportionally with the number of available adsorption sites, leading to a decrease in the amount adsorbed per unit mass and consequently a higher adsorption rate of ofloxacin. According to Hameed et al. (2009) and Yang et al. (2020), excess active sites cannot be occupied by the pollutant.

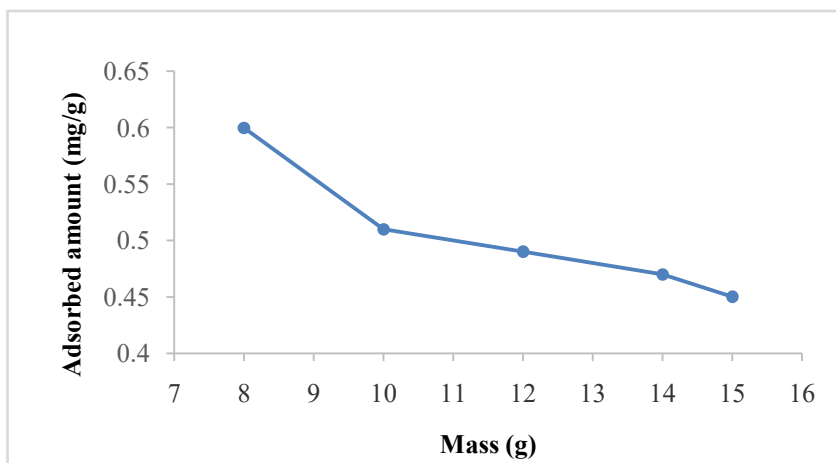


Figure 5: Effect of carbon mass on OFL adsorption, $C_o = 20$ mg/L; $V = 500$ mL; $pH = 6$

Effect of solution pH:-

Figure (6) illustrates the results of OFL adsorption on CAO at different solution pH values. The optimal pH ranges for OFL removal are between 5 and 6 (65.22% to 65.75%). At pH values above 6 (65.75–46.82%), a sharp drop in the adsorption rate is observed. These results could be attributed to the molecular structural characteristics of OFL and the pH_{zpc} of CAO. Indeed, OFL is an amphoteric molecule with ionisable functional groups. It has two pK_a values (pK_{a1}= 5.45 and pK_{a2}= 6.2) and can therefore exist in three forms in aqueous solution (Bhatia et al., 2016). The pH_{zpc} of CAO was determined to be 7.4. Thus, the surface of CAO is positively charged when the solution pH is < 7.4 and negatively charged when the pH is > 7.4. In an acidic medium, OFL is predominantly in its cationic form and the surface of the carbon is positively charged. As the surface charge of the material and the molecule are identical, this could lead to electrostatic repulsion. However, despite this phenomenon, the adsorption yield is found to be high. Indeed, repulsion is often dominated by other, stronger attractive forces such as Van der Waals forces (weak attraction due to electron fluctuations) or specific interactions (hydrogen bonding, ionic interactions). Thus, when these attractive forces are sufficiently strong, they can hold the molecule at the surface, leading to a high adsorption rate. Above pH 6, the dominant form of OFL is in the anionic state, resulting in adsorbent/adsorbate electrostatic repulsions, causing a decrease in adsorption capacity. A decrease in removal efficiency at higher pH has also been reported for the adsorption of fluoroquinolone antibiotics such as ciprofloxacin onto activated carbons (Ahmed and Theydan, 2014).

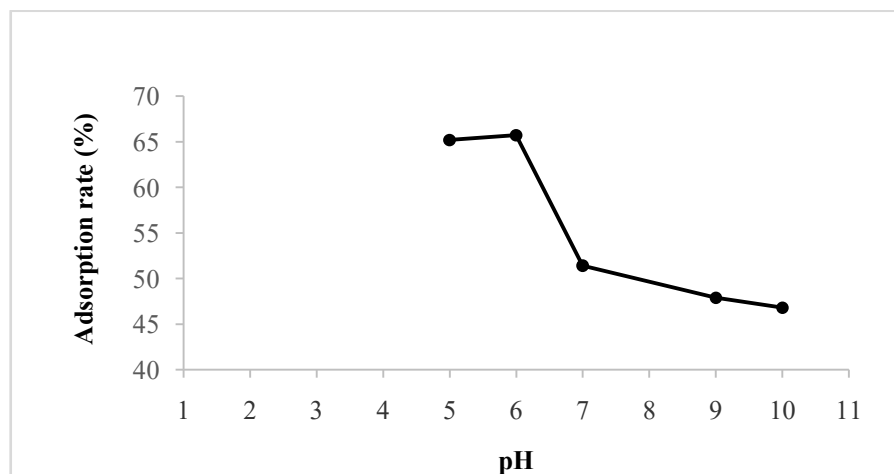


Figure 6: Effect of solution pH on OFL adsorption, $m = 4$ g; $V = 500$ mL and $C_o = 20$ mg/L

Effect of initial concentration:-

The results of the study on the effect of OFL concentration are presented in Figure (7). A similar trend is observed in the removal rate and the amount of OFL adsorbed. The amount adsorbed increases proportionally with the initial concentration. Indeed, when the initial concentration increases from 10 to 40 mg/L, the adsorption capacity increases from 0.34 to 0.62 mg/g. This increase could be explained by the fact that the increase in initial concentration provides a significant driving force, which accelerates the diffusion of the molecule across the surface of the adsorbent (Dhafir et al., 2014). The curve shows a plateau from 30 mg/L onwards, indicating saturation of the number of sites. Beyond this value, there is no further significant variation. Similar results have been reported in the literature (Dbik et al., 2014). With regard to the adsorption rate, an increase is observed up to 20 mg/L, corresponding to a 65.75% removal efficiency for OFL. Above this concentration, the adsorption rate decreases, indicating the gradual saturation of the carbon, which is thought to be due to the presence of excess OFL molecules relative to the active sites of the adsorbent (Tan et al., 2009).

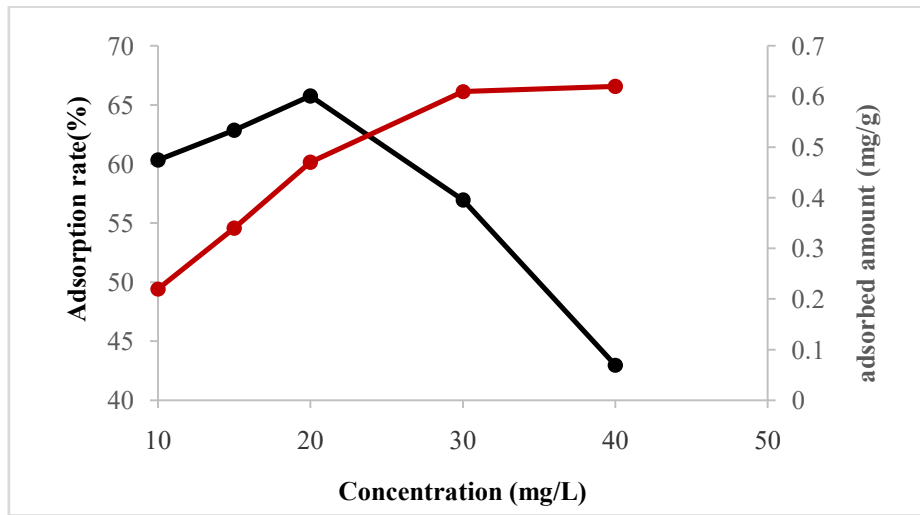
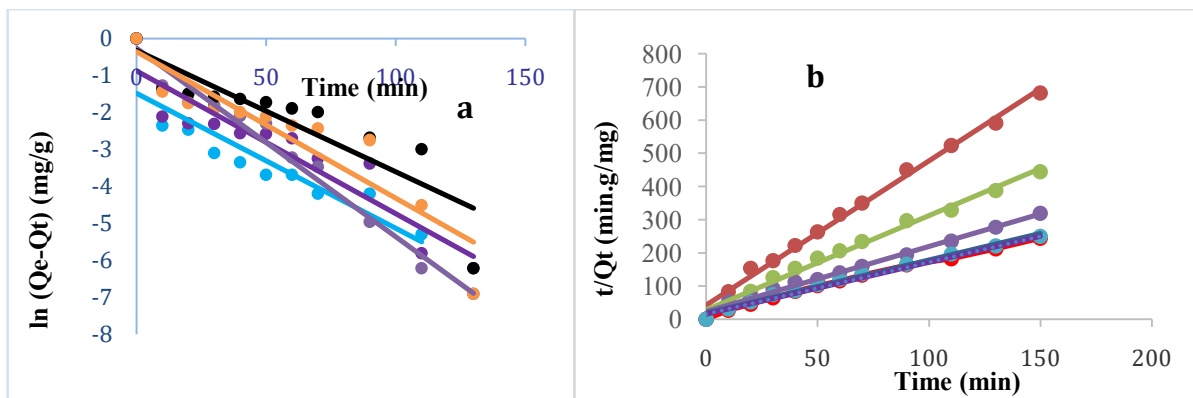


Figure 7: Effect of initial concentration on OFL adsorption, m = 4 g; V = 500 mL; pH = 6

Modelling of adsorption kinetics:-

Figure (8) presents the modelling of the experimental results for the adsorption kinetics of OFL on activated carbon.



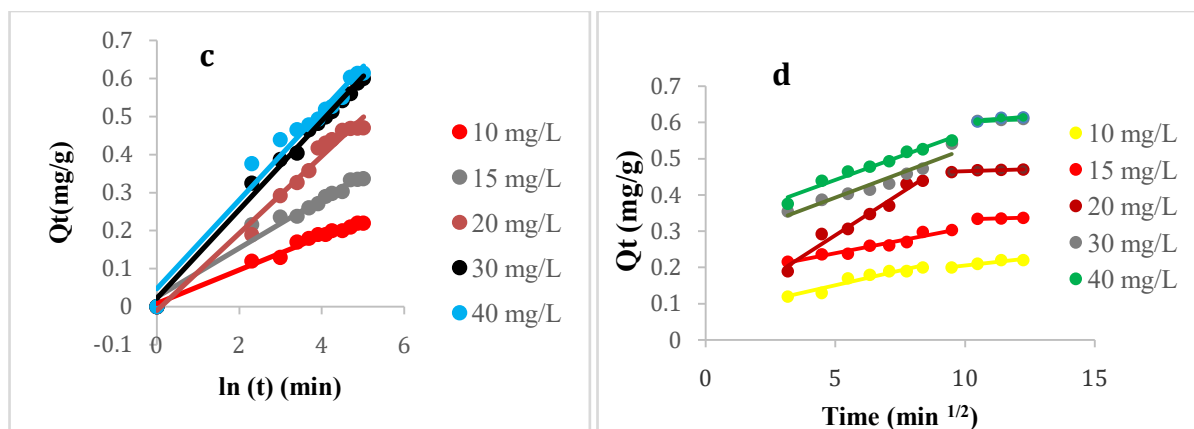


Figure 8: Kinetic models: (a): pseudo-first order, (b): pseudo-second order, (c): Elovich, (d): intraparticle diffusion

The main parameters characterising each model are summarised in Table (4).

Table (4): Kinetic parameters for the adsorption of OFL onto CAO

Co (mg/L)		10	15	20	30	40
Qe (mg/g) exp		0.22	0.34	0.47	0.61	0.61
Pseudo-first order	Qe (mg/g) cal	0.23	0.41	0.95	0.72	0.96
	K ₁ (min ⁻¹)	-	-0.00030	-0.00020	-0.00025	-0.00027
	R ²	0.84	0.81	0.87	0.97	0.77
Pseudo-second order	Qe (mg/g) cal	0.23	0.35	0.51	0.62	0.63
	K ₂ (mg.g ⁻¹ .min ⁻¹)	0.44	0.28	0.16	0.14	0.16
	R ²	0.99	0.99	0.99	0.99	0.99
Elovich	α (mg.g ⁻¹ .min ⁻¹)	0.11	0.14	0.09	0.15	0.11
	β (g/mg)	3.76	2.49	1.87	1.34	3.76
	R ²	0.98	0.96	0.98	0.99	0.97
Intraparticle diffusion	Qe (mg/g) cal	0.06	0.09	0.10	0.16	0.20
	K _{int} (mg.g.min ^{1/2})	0.016	0.023	0.038	0.043	0.042
	R ²	0.92	0.95	0.96	0.93	0.83

- ✓ With regard to the results of the pseudo-first-order model (Figure (8a), Table (4)), the coefficients of determination range from 0.77 to 0.97 and the constants (K₁) are all negative. Furthermore, the equilibrium adsorption capacity values theoretically determined by the pseudo-first-order model are almost all very different from the experimental values. This indicates that the pseudo-first-order model is entirely unsuitable for describing the adsorption kinetics of OFL.
- ✓ With regard to the pseudo-second-order model (Figure 8b, Table 4), the coefficients of determination (R²) are very close to 1 (R²= 0.99) for all initial concentrations. Furthermore, the equilibrium adsorption capacities calculated are close to the experimental values. The rate constants (K₂) are positive and range from 0.14 to 0.44. These results show that the pseudo-second-order model is more applicable to the adsorption kinetics of OFL.
- ✓ As for the Elovich model (Figure 8c, Table 4), the coefficients of determination range from 0.96 to 0.99. These relatively high values suggest that the surfaces of the coals are energetically heterogeneous (Rudzinski and Panczyk, 2002). The discrepancies between the theoretical and experimental adsorbed quantities (β) are very large, indicating that this model is not suitable for describing this process.
- ✓ According to the results of intraparticle diffusion (Figure 8d), it can be seen that, with regard to the linearisation of the model, the straight lines do not pass through the origin. This demonstrates that diffusion within the pores of the adsorbent is not the sole mechanism controlling the adsorption kinetics, but that it coexists with one or more other adsorption mechanisms (Sousa et al., 2012). This is confirmed by the presence of two straight lines for each concentration, thus proving the existence of two stages: the first stage represents diffusion of the external film and through the boundary layer of the outer surface of the activated carbon. It occurs during the first few minutes of

agitation, with a high adsorption rate. The second stage is intraparticle diffusion, characterised by a slowing of the adsorption rate. This is therefore the stage limiting the adsorption rate (Benammar, 2023). Examination of Table 4 shows that the values of the theoretical adsorbed quantities differ significantly from those obtained experimentally. The same applies to the correlation coefficients, whose values are not close to unity. The intraparticle diffusion model is therefore not suitable for describing the mechanism of OFL adsorption on CAO.

Modelling of adsorption isotherms:-

The adsorption isotherms of OFL on activated carbon are shown in Figure 9.

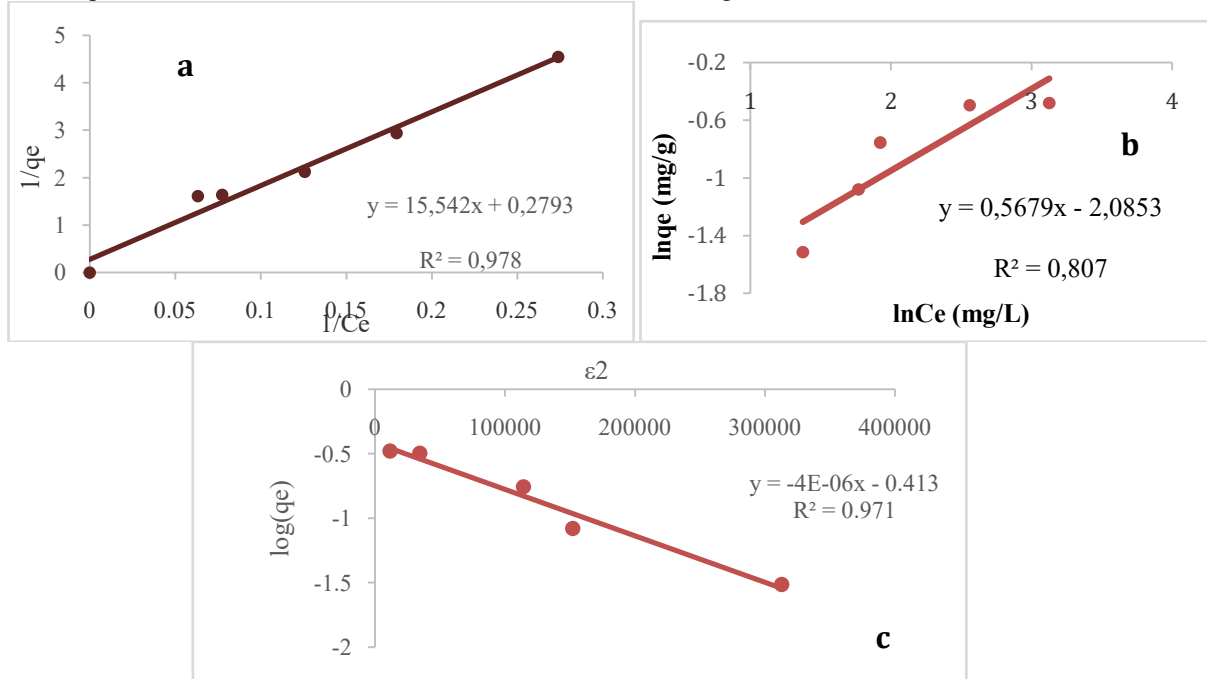


Figure 9: Modelling of the OFL adsorption isotherm on activated carbon: (a) ; (b): Freundlich model; (c): Dubinin-Radushkevich model

Table 5 presents the Langmuir and Freundlich constants obtained from the equations of these models.

Table (5): Parameters of the OFL adsorption isotherms on activated carbon

Langmuir				Freundlich			Dubinin-Radushkevich (D-R)		
Q _m (mg/g)	K _L	R _L (L/mg)	R ²	K _F	1/n _f	R ²	K _{DR} (mol ² .kJ ⁻²)	E (kJ.mol ⁻¹)	R
3,58	0,75	0,03	0,98	16,65	0,78	0,81	4. 10 ⁻⁶	0,35	0,97

Analysis of the results in this table reveals coefficients of determination of 0.98, 0.81 and 0.97 respectively for the Langmuir, Freundlich and Dubinin-Radushkevich models. The value of the Langmuir separation factor (R_L) is less than 1, indicating that adsorption is highly favourable for CAO. The adsorption energies obtained from the D-R model are all below 8 kJ/mol, indicating that the adsorption process is governed by a physisorption mechanism (Maji et al., 2007). Based on the R² values obtained, the Langmuir and Dubinin-Radushkevich models provide a better description of the nature of the adsorption. This suggests that the adsorption of molecules occurs on a homogeneous monolayer surface without interactions between the adsorbed molecules (Hameed et al., 2007).

Conclusion:-

This study demonstrated the effectiveness of activated carbon prepared from eggshells for the removal of ofloxacin from aqueous media. Characterisation of the activated carbon revealed a predominantly mesoporous material with a high specific surface area (5.429 m²/g) and a markedly basic character, with a pH_{pzc} of 7.4. The adsorption parameters

confirmed fairly good efficiency, with ofloxacin removal percentages of over 65% within 150 minutes. Adsorption is optimised at a pH of 6, with an adsorbent mass of 14 g and an initial ofloxacin concentration of 20 mg/L. The study of adsorption kinetics revealed that the pseudo-second-order model is appropriate for describing the adsorption process, with a regression coefficient R^2 very close to 1 ($R^2 = 0.99$). As for the adsorption isotherms, they are well represented by the Langmuir and Dubinin-Radushkevich models. Activated carbon derived from eggshells could be used as a means of treating water polluted by pharmaceutical residues.

References:-

1. Aboua, K.N. (2013). Optimisation of activated carbon production conditions using a full factorial design and its application for the removal of dyes and heavy metals from aqueous solutions. PhD thesis, Félix Houphouët-Boigny University, Abidjan, Côte d'Ivoire, 164 pp.
2. Adeyeye, E.I. (2009). Comparative study on the characteristics of egg shells of some bird species. International Journal of Chemical Sciences, 2(2), 191–201.
3. Ahmad, M., Rajapaksha, A.U., Lim, J.E., Zhang, M., Bolan, N., Mohan, D., Vithanage, M., Lee, S.S. & Ok, Y.S. (2014). Biochar as a sorbent for contaminant management in soil and water: a review. Chemosphere, 99, 19–33.
4. Ahmed, M.J. & Theydan, S.K. (2014). Adsorption of fluoroquinolone antibiotics on microporous activated carbon from lignocellulosic biomass by microwave pyrolysis. J. Taiwan Inst. Chem. Eng. 45, 219–226.
5. Al-Mardini, M. (2008). Study of the removal of organic micropollutants by adsorption on activated carbon: influence of natural organic matter. PhD thesis, University of Limoges, France.
6. Avom, J., Ketcba, M.J., Matip, M.R.L. & Germain, P. (2001). Adsorption isotherm of acetic acid by plant-based coals. African Journal of Science and Technology, 2(2), 1-7.
7. Benammar, H.S. (2023). Synergistic effects and adsorbent capacity of activated carbon in the removal of two azo dyes. PhD thesis, Mohamed Khider University – Biskra, 160 p.
8. Bhatia, V., Ray, A.K. & Dhir A. (2016). Enhanced photocatalytic degradation of ofloxacin by co-doped titanium dioxide under solar irradiation. Sep. Purif. Technol. 161, 1–7.
9. Bound, J.P. & Voulvoulis, N. (2005). Household disposal of unused and expired pharmaceuticals. Environmental Health Perspectives, 113(12), 1705–1711.
10. Brečević, L. & Nielsen, A.E. (1990). Precipitation of calcium carbonate: The formation of polymorphism. Journal of Crystal Growth, 102(1-2), 116-124.
11. Creangă, C.M. (2007). The AD-OX process for the removal of non-biodegradable organic pollutants (via adsorption followed by catalytic oxidation). PhD thesis, National Polytechnic Institute of Toulouse, France, 288 pp.
12. Dbik, A., El Messaoudi, N. & Lacherai, A. (2014). Utilisation of date stone wood from a palm variety in the Tinghir region (Morocco): Application to the removal of methylene blue. J. Mater. Environ. Sci., 5 (S2), 2510–2514.
13. Dhafir, T., Ajeel, A.H., Muna, A.R.K. & Omar, S.A. (2014). Adsorption of Ciprofloxacin Hydrochloride from Aqueous Solution by Iraqi Porcelinaite Adsorbent. Journal of Al-Nahrain University, Vol. 17 (1); pp. 41–49
14. Farcas, F. & Touzé, C. (2001). Characterisation of the constituents of civil engineering materials by infrared spectrometry. Bulletin des Laboratoires des Ponts et Chaussées, 230, 77–88.
15. Fierro, V., Torné-Fernández, Montané, D.V. & Celzard, A. (2008). Adsorption of phenol onto activated carbon with different textural and surface properties. Microporous and Mesoporous Materials, 111 (1-3): 276–284. <https://doi.org/10.1016/j.micromeso.2007.08.002>
16. Finqueneisel, G. (1998). Study of the surface chemistry of activated carbons: influence on adsorption and catalytic properties. PhD thesis, University of Metz, France.
17. Garcia-Prats, A.J., Achat, S.E., Osman, M., Draper, R.H., Schaaf, H.S., Wiesner, L., Denti, P. & Hesselring, A.C. (2019). Pharmacokinetics, safety and dosing of new paediatric dispersible levofloxacin tablets in children exposed to multidrug-resistant tuberculosis. Antimicrobial Agents and Chemotherapy, vol. 63, no. 4, pp. e01865-18–e01865-25
18. Giri, A.S. & Golder, A.K. (2015). Degradation of drug mixtures via Fenton and photo-Fenton processes: comparison with individual treatment, evolution of inorganic ions and toxicity. Chemosphere, 127, 254–261.
19. Guo, H.G., Gao, N.Y., Chu, W.H., Li, L., Zhang, Y.J., Gu, J.S. & Gu, Y.L. (2013). Photochemical degradation of ciprofloxacin in UV and UV/H₂O₂ processes: kinetics, parameters and products. Environ. Sci. Pollut. Rem. 20, 3202–3213.
20. Gupta, A. & Garg, A. (2018). Degradation of ciprofloxacin using Fenton oxidation: effect of operating parameters, identification of oxidation by-products and toxicity assessment. Chemosphere, 193, 1181–1188.

21. 20. Habeeb, O.A., Yasin, F.M. & Danhassan, U.A. (2014). Characterisation and application of chicken eggshell as green adsorbents for the removal of H₂S from wastewaters. *Journal of Environmental Science, Toxicology and Food Technology*, vol. 8, 7–12.
22. Hameed, B.H., Ahmad, A.L. & Latiff, K.N.A. (2007). Adsorption of basic dye (methylene blue) on activated carbon prepared from rattan sawdust. *Dyes and Pigments*, 75:143–149.
23. Hameed, B.H., Tan, I.A.W. & Hamad, A. (2009). Preparation of oil palm empty fruit bunch-based activated carbon for the removal of 2,4,6-trichlorophenol: optimisation using response surface methodology. *Journal of Hazardous Materials*, 164, 1316–1324.
24. Horsfall, M. & Spiff, A.I. (2004). Studies on the influence of liquid phase variables on the adsorption of heavy metal ions (Zn²⁺, Cu²⁺ and Cd²⁺) from aqueous solutions by cassava (*Manihot esculenta* Cranz) tuber bark waste. *Bioresource Technology*, 93(3), 277–283.
25. Kummerer, K. (2009). Antibiotics in the aquatic environment. A review. *Chemosphere*, 75(4), 417–434.
26. Leipert, J., Bobis, I., Schubert, S., Fickenscher, H., Leippe, M. & Tholey, A. (2018). Miniaturised dispersive liquid-liquid microextraction and MALDI MS using ionic liquid matrices for the detection of bacterial signalling molecules and virulence factors. *Analytical and Bioanalytical Chemistry*, vol. 410, pp. 4737–4748.
27. Liu, C., Nanaboina, V., Korshin, G.V. & Jiang, W. (2012). Spectroscopic study of the degradation products of ciprofloxacin, norfloxacin and lomefloxacin formed in ozonated wastewater. *Water. Water Res.*, 46, 5235–5246 .
28. Maji, S.K., Pal, A., Pal, T. & Adak, A. (2007). Adsorption thermodynamics of arsenic on laterite soil. *J. Surface Sci. Technol.* 22 (3-4): 161–176.
29. Mohadi, R., Anggraini, K., Riyanti, F. & Lesbani, A. (2016). Preparation, Characterisation and Application of Eggshell as a Low-Cost Adsorbent for the Removal of Congo Red from Aqueous Solution. *Journal of Chemical and Pharmaceutical Research*, 8(4), 301–308.
30. Nahil, M.A. & Williams, P.T. (2012). Pore characteristics of activated carbons from the phosphoric acid chemical activation of cotton stalks. *Biomass and Bioenergy*, vol. 37, 142–149.
31. Omokpariola, D.O. (2021). Application of Weber-Morris and Boyd diffusion models in the adsorption of heavy metals: A review. *Scientific Journal of Pure and Applied Sciences*, 10(2), 654–663.
32. Patil, A. & Shrivastava, V. (2010). Alternanthera bettzichiana plant powder as a low-cost adsorbent for the removal of Congo red from aqueous solution. *Int. J. Chemtech Res.* 2:842–850.
33. Pilecki, Z., Pilecka, E. & Szarek-Gwiazda, E. (2019). The importance of Fourier-transform infrared spectroscopy in the identification of carbonate phases with variable magnesium content. *Spectroscopy*, 34(6), 32–38.
34. Rivera-Utrilla, J., Sanchez-Polo, M., Ferro-Garcia, M.A., Pardos-Joya, G. & Ocampo-Perez, R. (2013). Pharmaceuticals as emerging contaminants and their removal from water: a-review. *Chemosphere*, 93, 1268–1287
35. Rudzinski, W. & Panczyk, T. (2002). The Langmuir adsorption kinetics revised: a farewell to 20th-century theories. *Adsorption*, 8(1): 23–34.
36. Samarghandi, M. R., Hadi, M., Moayedi, S. & Barjasteh, A.F. (2009). Two-parameter isotherms of methyl orange sorption by pinecone-derived activated carbon. *Iran. J. Environ. Health. Sci. Eng.* Vol. 6, No. 4, pp. 285–294.
37. Shi, S., Fan, Y. & Huang, Y. (2013). Simple low-temperature hydrothermal synthesis of mesoporous magnetic carbon nanocomposites for the adsorption-based removal of ciprofloxacin Antibiotics. *Chemical Resolution Independent eng.* 52, 2604–2612 .
38. Skoog, D.A., Holler, F.J. & Crouch, S.R. (2018). Principles of Instrumental Analysis. Cengage Learning. *Chemical Engineering*, 8(1), 103565.
39. Sogbochi, E. (2023). Thermochemical preparation of activated carbons derived from , a by-product of *Lophira lanceolata*: adsorption tests for water micropollutants. PhD thesis, University of Abomey-Calavi, 176 pp.
40. Sousa, N.V.O., Tecia, V.C., Honorato, S.B., Gomes, C.L., Baros, F.C.F., Araujo-Silvia, M.A., Freire, P.T.C. & Nascimento, R.F. (2012). Coconut bagasse treated with thiourea/ammonia solution for cadmium removal: kinetics and adsorption equilibrium. *BioResource*, 7, 1504–1524.
41. Tan, I.A., Ahmad, A.L. & Hameed, B. H. (2009). Adsorption isotherms, kinetics, thermodynamics and desorption studies of 2, 4, 6-trichlorophenol on oil palm empty fruit bunch-based activated carbon. *J. Hazard. Mater.* 164, 473–482.
42. Yang, L., Zhou Y., Shi B., Meng J., Il B., Yang H. & Yoon S.J. (2020). Anthropogenic impacts on the contamination of pharmaceutical and personal care products (PPCPs) in the coastal environments of the Yellow Sea and Bohai Sea. *Environ. Int.* 135, 105306.